The Journal of Immunology

Mycobacterium bovis Bacillus Calmette-Guérin Induces TLR2-Mediated Formation of Lipid Bodies: Intracellular Domains for Eicosanoid Synthesis In Vivo

Heloisa D'Avila, Rossana C. N. Melo, Gleydes G. Parreira, Eduardo Werneck-Barroso, Hugo C. Castro-Faria-Neto and Patrícia T. Bozza

J Immunol 2006; 176:3087-3097; ;
doi: 10.4049/jimmunol.176.5.3087
http://www.jimmunol.org/content/176/5/3087

The Journal of Immunology is published twice each month by
The American Association of Immunologists, Inc.,
1451 Rockville Pike, Suite 650, Rockville, MD 20852

Print ISSN: 0022-1767 Online ISSN: 1550-6606.

Mycobacterium bovis Bacillus Calmette-Guérin Induces TLR2-Mediated Formation of Lipid Bodies: Intracellular Domains for Eicosanoid Synthesis In Vivo[1]

Heloisa D'Avila,* Rossana C. N. Melo,† Gleydes G. Parreira,‡ Eduardo Werneck-Barroso,§ Hugo C. Castro-Faria-Neto,* and Patrícia T. Bozza[2]*

Differentiation of macrophages into foamy (lipid-laden) macrophages is a common pathological observation in tuberculous granulomas both in experimental settings as well as in clinical conditions; however, the mechanisms that regulate intracellular lipid accumulation in the course of mycobacterial infection and their significance to pathophysiology of tuberculosis are not well understood. In this study, we investigated the mechanisms of formation and function of lipid-laden macrophages in a murine model of tuberculosis. *Mycobacterium bovis* bacillus Calmette-Guérin (BCG), but not *Mycobacterium smegmatis*, induced a dose- and time-dependent increase in lipid body-inducible nonmembrane-bound cytoplasmic lipid domain size and numbers. Lipid body formation was drastically inhibited in TLR2-, but not in TLR4-deficient mice, indicating a role for TLR2 in BCG recognition and signaling to form lipid bodies. Increase in lipid bodies during infection correlated with increased generation of PGE_2 and localization of cyclooxygenase-2 within lipid bodies. Moreover, we demonstrated by intracellular immunofluorescent localization of newly formed eicosanoid that lipid bodies were the predominant sites of PGE_2 synthesis in activated macrophages. Our findings demonstrated that BCG-induced lipid body formation is TLR2 mediated and these structures function as signaling platforms in inflammatory mediator production, because compartmentalization of substrate and key enzymes within lipid bodies has impact on the capacity of activated leukocytes to generate increased amounts of eicosanoids during experimental infection by BCG. *The Journal of Immunology,* 2006, 176: 3087–3097.

Mycobacteria are the etiologic agents of numerous diseases that account for significant morbidity and mortality in humans and different animal species. Tuberculosis alone is responsible for almost 3 million deaths annually worldwide. Members of the *Mycobacterium tuberculosis* complex, comprised by *M. tuberculosis*, *Mycobacterium bovis*, and *Mycobacterium africanum*, are the etiologic agents of the human and animal tuberculosis (1).

Macrophage activation determines the outcome of mycobacterial infection. All pathogenic *Mycobacterium spp.* survive as intracellular pathogens within host phagocytes, in part by modulating the phagosomal compartment to prevent its maturation and subsequent acidification (2, 3). The mechanisms that allow intracellular pathogens to avoid destruction are still not completely understood. There is a growing body of evidence pointing to an important modulatory role of bacterial- and host-derived lipids in mycobacterial infection (2–6).

Differentiation of macrophages into foamy macrophages is a common pathological observation in tuberculous granulomas both in experimental settings as well as in clinical conditions (7–9). As observed for other pathological conditions, the foam aspect of macrophages is a reflex of intracellular lipid accumulation. However, mechanisms that regulate intracellular lipid accumulation in the course of mycobacterial infection and their significance to pathophysiology of tuberculosis are not completely understood. In different cell types, including leukocytes, intracellular lipids are stored in hydrophobic organelles called lipid bodies or lipid droplets. Cytoplasmic lipid bodies are osmiophilic structures, surrounded by a phospholipid monolayer with a unique fatty acid composition, have a neutral lipid rich core, and contain a variable protein composition (10–12). Recent studies based on lipid body proteic content have suggested that lipid bodies are dynamic and functionally active organelles. Among a growing list of proteins found within lipid bodies, they compartmentalize fatty acid metabolic enzymes, eicosanoid-forming enzymes, proteins of the Rab family, specific kinases, and small GTPases (13–21). Therefore, lipid bodies may regulate lipid metabolism, membrane trafficking, intracellular signaling, and inflammatory mediator production. In fact, in inflammatory leukocytes, arachidonic acid (AA),[3] an important signaling molecule and also precursor to inflammatory lipid mediators, is stored in its esterified form at lipid bodies (16, 22, 23).

*Laboratório de Imunofarmacologia, Departamento de Fisiologia e Farmacodinâmica, Instituto Oswaldo Cruz, Fundação Oswaldo Cruz, Rio de Janeiro, RJ, Brazil; †Laboratório de Biologia Celular, Departamento de Biologia, Universidade Federal de Juiz de Fora, Juiz de Fora, Minas Gerais, Brazil; ‡Departamento de Morfologia, Universidade Federal de Minas Gerais, Belo Horizonte, Minas Gerais, Brazil; and §Laboratório de Farmacocinética, Fundação Oswaldo Cruz, Rio de Janeiro, RJ, Brazil

Received for publication April 6, 2005. Accepted for publication December 9, 2005.

The costs of publication of this article were defrayed in part by the payment of page charges. This article must therefore be hereby marked *advertisement* in accordance with 18 U.S.C. Section 1734 solely to indicate this fact.

[1] This work was supported by Howard Hughes Medical Institute (to P.T.B.), Programa Núcleos de Excelência-Ministério da Ciência e Tecnologia, Conselho Nacional de Desenvolvimento Científico e Tecnológico (CNPq-Brazil), and Fundação de Amparo à Pesquisa do Rio de Janeiro.

[2] Address correspondence and reprint requests to Dr. Patricia T. Bozza, Laboratório de Imunofarmacologia, Departamento de Fisiologia e Farmacodinâmica, Instituo Oswaldo Cruz, Fundação Oswaldo Cruz, Avenida Brazil 4365, Manguinhos, Rio de Janeiro, RJ, Brazil - 21045-900. E-mail address: pbozza@ioc.fiocruz.br

[3] Abbreviations used in this paper: AA, arachidonic acid; ADRP, adipose differentiation-related protein; BCG, bacillus Calmette-Guérin; COX, cyclooxygenase; EDAC, 1-ethyl-3(3-dimethylamino-propyl) carbodiimide; EIA, enzyme-linked immunoassay; i.pl., intrapleural; LAM, lipoarabinomannan; LT, leukotriene; MOI, multiplicity of infection; NSAID, nonsteroidal anti-inflammatory drug; RT, room temperature.

0022-1767/06/$02.00

AA and its oxygenated lipid metabolites have been implicated as important molecules in host response to mycobacterial infection (4, 24). Indeed, free AA is able to stimulate actin nucleation and phagosome maturation in infected cells with a direct impact on intracellular pathogen survival within the macrophage (4). Moreover, infection of macrophages with *M. tuberculosis* induces activation of cytosolic phospholipase A_2, leading to increased levels of free AA, initiation of apoptosis, and antimycobacterial activity, phenomena that could be reproduced by adding exogenous free AA. In sharp contrast, the enzymatic conversion of free AA into PGs or lipoxins down-modulates cell-mediated response to intracellular pathogens favoring pathogen burden (25–27). Therefore, one important issue in understanding the molecular mechanisms of innate immunity to intracellular parasites is the regulation of the production of lipid mediators such as eicosanoids.

In the present study, we used a murine model of pleural tuberculosis to demonstrate that mycobacterial infection induces lipid body formation in a tightly regulated manner that is largely dependent of TLR2 signaling. Moreover, we demonstrated that newly formed lipid bodies are structurally distinct intracellular sites for lipid mediator synthesis with paracrine and/or intracrine functions during bacillus Calmette-Guérin (BCG) infection.

Materials and Methods

Abs and reagents

Mouse anti-PGE_2, aspirin (acetyl salicylic acid), NS-398, and PGE_2 enzyme-linked immunoassay (EIA) kit were purchased from Cayman Chemical. Rabbit polyclonal anti-mouse cyclooxygenase-2 (COX-2) was purchased from Oxford Biomedical Research. Biotin-conjugated goat anti-rabbit IgG, nonimmune rabbit serum, and Vectastain glucose-oxidase kit were obtained from Vector Laboratories. Guinea pig polyclonal anti-mouse adipose differentiation-related protein (ADRP) was purchased Research Diagnostics. CY3-conjugated donkey anti-guinea pig was obtained from Jackson ImmunoResearch Laboratories. IgG1 isotype control (MOPC 21), 1-ethyl-3(3-dimethylamino-propyl) carbodiimide (EDAC), 4′-6′-diamidino-2-phenylindole, indomethacin, LPS from *Escherichia coli* (serotype 0127:b8), and Nile Red were purchased from Sigma-Aldrich. Goat anti-mouse conjugated with AlexaFluor-488, 1-acyl-2-(7-octyl BODIPY-1-pentanoyl)-*sn*-glycerol, Live/Dead BacLight bacterial viability kit, and latex beads were obtained from Molecular Probes. Calcium ionophore A23187 was purchased from Calbiochem-Novabiochem. Osmium tetroxide was obtained from Merck. A multiplex cytokine kit was obtained from Upstate Biotechnology.

Animals

C57BL/6 (B6) and C3H/HeN mice were obtained from the Fundação Oswaldo Cruz breeding unit. C3H/HeJ, C57BL/10 ScSn, and C57BL/10 ScCr (TLR4-deficient mice) were obtained from Universidade Federal Fluminense. TLR2 knockout mice in a homogeneous B6 background (28) were donated by S. Akira (Osaka University, Osaka, Japan), MCP-1/CCL2-deficient mice in a mixed B6 and 129Sv/J genetic background and wild-type littermates (29) were provided by C. Gerard (Harvard Medical School, Boston, MA), and TNFRI (p55)-deficient mice in a homogeneous B6 background were obtained from The Jackson Laboratory. Animals were bred and maintained under standard conditions in the breeding unit of the Oswaldo Cruz Foundation. Animals were caged with free access to food and water in a room at 22–24°C and a 12-h light/dark cycle in the Department of Physiology and Pharmacodynamic animal facility until used. Animals weighing 20–25 g from both sexes were used. All protocols were approved by the Fundação Oswaldo Cruz animal welfare committee.

Bacterial strains

M. bovis BCG (Moreau strain) vaccine was donated by Fundação Athaulpho de Paiva (30). The freeze-dried vaccine was stored at 4°C and resuspended in physiologic solution just before use. *Mycobacterium smegmatis* (mc^2155) and *Bacillus subtilis* (PY79) were stored at −70°C and resuspended in physiologic solution just before use.

In vitro infection

Peritoneal cells from naive B6 mice were harvested by lavage with sterile RPMI 1640 cell culture medium. Macrophages (1×10^6 cells/ml) were adhered in cover slides within culture plates (24 wells) overnight with RPMI 1640 cell culture medium containing 2% FCS. The nonadherent cells were removed after vigorous PBS wash (twice). Macrophages were infected by BCG (multiplicity of infection (MOI), 1:1), *M. smegmatis* (MOI, 5:1), or *B. subtilis* (1:1), or stimulated with latex beads (1:1), zymozan (1:1), LPS (500 ng/ml), or lipoarabinomannan (LAM; 500 ng/ml) for 24 h at 37°C in CO_2 atmosphere. In inhibitory studies, macrophages were infected by BCG (MOI, 5:1) for 1 h, followed by PBS wash (three times) to remove noninternalized BCG. Then, the cells were treated with aspirin (5 μM) or NS-398 (1 μM) for 24 h at 37°C. Vehicle (0.01% DMSO) was used as control. Viability was assessed by trypan blue exclusion at the end of each experiment and was always >90%.

Pleurisy induced by BCG or M. smegmatis

Mice were intrapleurally (i.pl.) injected with BCG (5×10^5 bacilli/cavity or 5×10^6 bacilli/cavity) or *M. smegmatis* (5×10^6 bacilli/cavity) in 100 μl of sterile saline. Control animals received an equal volume (100 μl) of sterile saline only. After different time intervals (1 h to 15 days), the animals were killed by CO_2 inhalation, and their thoracic cavities were washed with 1 ml of the heparinized PBS (10 UI/ml).

Electron microscopy

Pleural cells from control and infected animals (5×10^6 of BCG/cavity for 1 and 24 h) were centrifuged (2000 rpm, 5 min), and the pellets obtained were resuspended and fixed in a mixture of freshly prepared aldehydes (1% paraformaldehyde and 1% glutaraldehyde) in 0.1 M phosphate buffer (pH 7.3) overnight at 4°C (31). The cells were washed in the same buffer and embedded in molten 2% agar (Merck). Agar pellets containing the cells were postfixed in a mixture of 1% phosphate-buffered osmium tetroxide and 1.5% potassium ferrocyanide (final concentration). Cells were dehydrated and embedded in Epon (PolyBed 812; Polysciences). The sections were mounted on uncoated 200-mesh copper grids (Ted Pella) before staining with uranyl acetate and lead citrate and viewed with a transmission electron microscope (EM 10; Zeiss) at 60 KV.

Lipid body staining and enumeration

Different techniques were used for lipid body staining and quantification. For most studies, cells were stained by osmium tetroxide and numerated exactly as described (32). For fluorescent labeled lipid bodies, cells recovered from the pleural cavities after 24 h of the infection by BCG and controls were incubated with 1 μM fluorescent fatty acid-containing diglyceride, 1-acyl-2-(7-octyl BODIPY-1-pentanoyl)-*sn*-glycerol for 1 h at 37°C or with Nile Red (1/10,000 from a stock solution of 0.1 mg/ml in acetone). After incubation, cells were washed twice in Ca^{2+}/Mg^{2+}-free HBSS ($HBSS^{-/-}$), cytospun onto slides, and fixed in 3.7% formaldehyde at room temperature (RT) for 10 min.

Fluorescent-labeled BCG

BCG (50×10^6 bacilli/ml) was incubated with 3 μl of the component A (Live/Dead BacLight bacterial viability kit) and incubated at RT in the dark for 15 min. BCG was pelleted by centrifugation, washed, and resuspended in physiologic solution. Animals were infected i.pl. by fluorescent labeled BCG (5×10^6 bacilli/cavity). Twenty-four hours after infection, the animals were killed, and pleural cells (1×10^5) were fixed in 3.7% formaldehyde for 10 min, washed, incubated with Nile Red for lipid body staining, rinsed three times in water, mounted, and examined under fluorescence microscopy, using a ×100 objective lens.

Phagocytic index

Phagocytic index was evaluated in cells from infected mice after mycobacterial staining by Kinyoun's acid fast staining method. In brief, cytocentrifuged smears were fixed in methanol and stained with Kinyoun's carbol fuchsin, as described (33). The cells were observed under light microscopy in a ×100 objective lens. The results were expressed as percentage of infected cell.

COX-2 immunolocalization

Cytocentrifuged smears were fixed in 3.0% formaldehyde at RT for 10 min, permeabilized with 0.05% saponin/$HBSS^{-/-}$ solution (5 min), and then blocked with 10% normal goat serum. After washing, slides were incubated for 1 h at RT with anti-COX-2 (1/150) polyclonal Abs diluted in 0.05% saponin/HBSS solution. Nonimmune rabbit serum (1/150) was used as control. After three washes of 5 min, the preparations were incubated for 1 h at RT with the secondary Ab, biotin-conjugated goat anti-rabbit IgG. The cell immunoreactivity was then identified by ABC Vectastatin glucose-oxidase kit, per the manufacturer's instructions. The glucose-oxidase

immunostaining and fluorescent lipid bodies were visualized under bright and fluorescent microscopy, respectively.

Immunodetection of PGE_2 at its sites of production

Immunolocalization of PGE_2 at its in vivo formation sites within infected macrophages was performed, as described (34, 35), and modified, as follows. Briefly, cells obtained 24 h after infection with BCG and controls were recovered from the thoracic cavity with 500 μl of HBSS, and immediately mixed with 500 μl of water-soluble EDAC (1% in HBSS), used to cross-link eicosanoid carboxyl groups to amines in adjacent proteins. After 15- to 30-min incubation at 37°C with EDAC to promote both cell fixation and permeabilization, pleural leukocytes were then washed with HBSS, cytospun onto glass slides, and incubated with mouse anti-PGE_2 (1/100) in 0.1% normal goat serum and guinea pig polyclonal anti-mouse ADRP (1/1000) in 0.1% normal donkey serum simultaneously for 1 h at RT. MOPC 21 and nonimmune guinea pig serum were used as controls. Cells were washed twice and incubated with secondary Abs, goat anti-mouse conjugated with AlexaFluor-488 (1/1000), and CY3-conjugated donkey anti-guinea pig (1/1000). The slides were washed (three times, 10 min each) and mounted with aqueous mounting medium (Polysciences). Cells were analyzed by both phase-contrast and fluorescence microscopy. As a control for PGE_2 specificity of detection, one group of BCG-infected animals was treated with indomethacin (4 mg/kg) 4 h before sacrificing the animals for cell recovery.

PGE_2 measurement

PGE_2 levels were measured directly in the supernatant from cell-free pleural lavage obtained 1 or 24 h after saline or BCG injection. In priming studies, pleural cells, stimulated as described above, were obtained for lipid body enumeration. Cells were washed in $HBSS^{-/-}$. Pleural cells (1×10^6 cells/ml) were resuspended in HBSS containing Ca^{2+}/Mg^{2+} and then stimulated with A23187 (0.5 μM) for 15 min. Reactions were stopped on ice, and samples were centrifuged at $500 \times g$ for 10 min at 4°C. PGE_2 was assayed in the cell-free supernatant by EIA, according to the manufacturer's instructions (Cayman Chemical).

Cytokine analysis

Supernatants from in vitro BCG-infected macrophages after 24 h of infection were collected and stored at −20°C until the day of analysis. TNF-α and IL-10 were analyzed simultaneously using luminex technology. A mouse multiplex cytokine kit was obtained, and the assay was performed according to the manufacturer's instructions (Upstate Biotechnology). A total of 50 μl of sample was analyzed on the Bio-Plex system (Bio-Rad), according to the manufacturer's instructions. Data analyses of all assays were performed with the Bio-Plex Manager software.

Image acquisition

The images were obtained using an Olympus BX-FLA fluorescence microscope equipped with a Plan Apo 100 × 1.4 Ph3 objective (Olympus Optical) and CoolSNAP-Pro CF digital camera in conjunction with Image-Pro Plus version 4.5.1.3 software (Media Cybernetics). The images were edited using Adobe Photoshop 5.5 software (Adobe Systems).

Statistical analysis

The results were expressed as mean ± SEM and were analyzed statistically by means of ANOVA, followed by the Neuman-Keuls-Student's test, with the levels of significance set at $p < 0.05$.

Results

M. bovis *BCG induces lipid body formation during in vivo infection*

Mechanisms involved in lipid body formation within *Mycobacterium*-infected cells were investigated using an experimental model of mouse pleurisy induced by *M. bovis* BCG, which allows the assessment of the acute inflammatory process induced by mycobacterial infection. Fig. 1 shows that cells from BCG-infected animals, appropriately treated for lipid fixation and staining, contain markedly increased numbers of lipid bodies at 1 (Fig. 1*B*) and 24 h (Fig. 1*C*) when compared with control (Fig. 1*A*). Alcohol-based fixation, as in Kinyoun's staining, causes dissolution of lipid bodies (Fig. 1*D*), which precludes their recognition in BCG-stimulated leukocytes and confers a foamy-like aspect to the cell. We observed that BCG induced a dose-dependent increase on lipid body formation, with maximum lipid body induction observed at the dose of 5×10^6 CFU/cavity (Fig. 1*F*). Lipid body formation initiated within 1 h reached maximum levels within 24 h and remained significantly increased 15 days after infection (Fig. 1*E*). The i.pl. injection of BCG (5×10^6 CFU/cavity) in B6 induced leukocyte accumulation with similar kinetic of that of the lipid body formation. The first phase was characterized by a marked increase in neutrophil numbers (1–6 h). At 24 h, a peak in the total leukocyte number was observed due to increase in eosinophil, macrophage, and lymphocyte numbers, and leukocytes remained increased after 15 days of infection (data not shown), as previously demonstrated (36, 37).

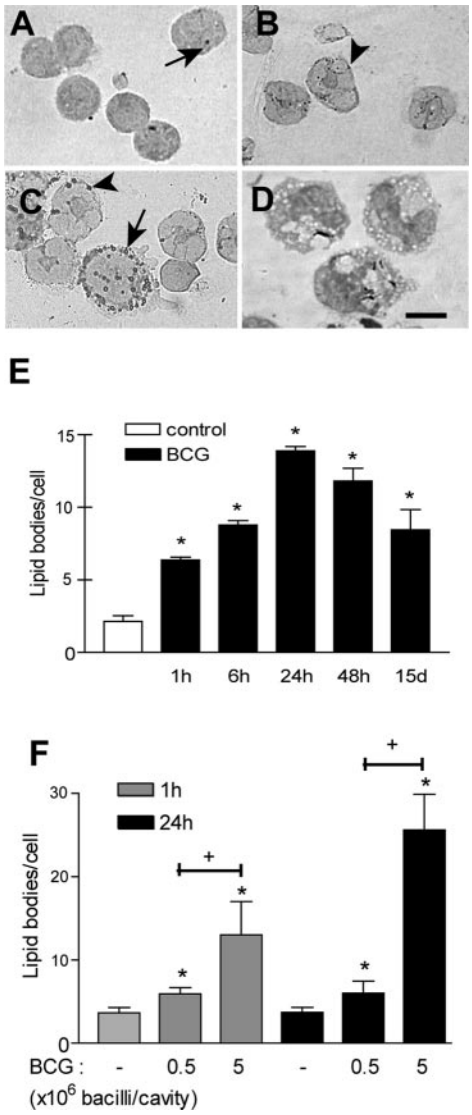

FIGURE 1. BCG infection induces time- and dose-dependent lipid body formation in pleural cells. Macrophage (arrow) and neutrophil (arrowhead) lipid bodies after osmium staining observed in control (*A*) or BCG-infected mice within 1 h (*B*) or 24 h (*C*). *D*, Macrophages from infected mice at 24 h of infection after Kinyoun's staining exhibit foamy cell-like morphology. Bars, 10 μm. *E*, Kinetic of BCG-induced lipid body formation in pleural cells. B6 mice were i.pl. infected with BCG (5×10^6 bacilli/cavity). *F*, Dose-response analysis of BCG-induced lipid body formation in pleural cells after 1 and 24 h of i.pl. injection of BCG. Each bar represents the mean ± SEM from 50 consecutively counted leukocytes from at least eight animals. Statistically significant ($p < 0.05$) differences are indicated by asterisks or +.

Increased lipid body formation was observed in both macrophages and neutrophils following BCG infection in vivo. However, more pronounced increases in the size as well as in the numbers of lipid bodies were noted in macrophages. In neutrophils, the number of lipid bodies increased within 1 h and was maximal within 24 h (mean ± SEM; from 1.66 ± 1.2 lipid bodies/neutrophil in control to 8.5 ± 0.66 lipid bodies/neutrophil at 1 h, and 11.5 ± 1.1 lipid bodies/neutrophil within 24 h). Although macrophages exhibited a modest increase at 1 h (from 0.3 ± 0.3 lipid bodies/macrophage in control to 4.0 ± 0.57 lipid bodies/macrophage), dramatic increments in the numbers of lipid bodies were observed at 24 h (27.0 ± 1.28 lipid bodies/macrophage).

Mycobacterium-*induced lipid bodies are morphologically distinct cytoplasmic sites*

To study the ultrastructure of BCG-elicited lipid bodies, pleural cells were immediately fixed while still in suspension in a mixture of glutaraldehyde and paraformaldehyde, embedded in agar, and prepared for conventional transmission electron microscopy. Because lipid bodies are nonmembrane-bound structures, cells were processed for optimal membrane visualization with the reduced osmium potassium ferrocyanide method, so as to distinguish lipid bodies from membranous organelles.

After 1 h of infection, macrophages showed cytoplasmic lipid bodies imaged as strongly osmiophilic structures localized mainly in the cell periphery (Fig. 2, *B*, *E*, and *F*), morphologically similar to lipid bodies from control cells (Fig. 2, *A* and *D*). After 24 h of infection, lipid bodies became large and light dense structures with a frequent peripheral rim of electron-dense material (Fig. 2, *C*, *H*, and *I*). In addition, they had eccentric or central lucent areas (Fig. 2*H*). Electron microscopy quantitative analyses showed a dramatic increase in lipid body size after 24 h of infection compared with 1 h (Fig. 2*J*). The number of lipid bodies per cell section was significantly increased (mean ± SEM; from 0.8 ± 0.2 lipid bodies/section in control to 2.6 ± 0.3 lipid bodies/section at 1 h, and 3.0 ± 0.2 lipid bodies/section within 24 h), as also shown by light microscopy (Fig. 1*E*). Images suggesting fusion of lipid bodies with each other were observed in macrophages at both 1 and 24 h after infection (Fig. 2, *E* and *I*, respectively). Remarkably, lipid bodies from infected animals showed clear interaction with phagosomes (Fig. 2*G*).

Mechanisms of lipid body formation in BCG-infected animals

The need of bacterial phagocytosis to lipid body formation was analyzed. The lack of correlation between bacterial phagocytosis and lipid body formation was suggested by the comparison of percentages of infected cells (attested by Kinyoun's staining) and percentages of cells with increased lipid body numbers within 24 h of BCG injection. As observed in Fig. 3*A*, 96% of leukocytes recovered from vehicle-stimulated cavities had <5 lipid bodies/cell, whereas after 24 h of BCG administration >95% of cells had ≥10 lipid bodies. In contrast, <30% of the cells had detectable phagocytosed bacteria within 24 h of BCG administration (Fig. 3*B*). In addition, by infecting the animals with fluorescent labeled BCG and labeling lipid bodies with Nile Red (a neutral lipid marker), we observed both infected cells with many cytoplasmic lipid bodies as well as uninfected cells with increased lipid body numbers (Fig. 3*C*), suggesting that mechanisms involved in lipid body formation were independent of bacterial ingestion.

To ascertain whether the observed lipid body formation in macrophages is a phagocytic-dependent phenomenon, peritoneal macrophages were incubated either with inert latex beads, *B. subtilis*, or BCG-derived LAM. As shown in Fig. 3*D*, macrophage stimulation with latex beads (1:1) or with *B. subtilis* (1:1) failed to induce lipid body formation within 24 h, thus indicating that not any phagocytic stimuli is capable of triggering mechanisms of lipid body induction.

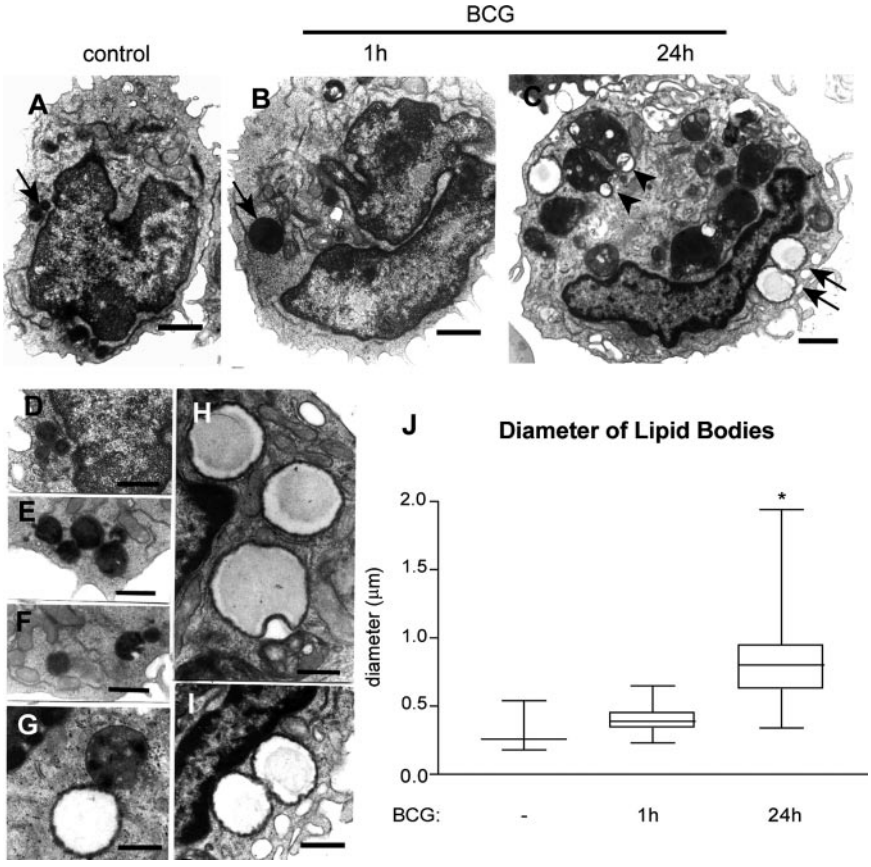

FIGURE 2. BCG-induced lipid bodies are morphologically distinct cytoplasmic sites. *A*, Control macrophage with typical morphology and small lipid bodies (arrow) in the cytoplasm. At 1 h (*B*) and 24 h (*C*) of infection, macrophages showed morphological pattern of activation and large cytoplasmic lipid bodies (arrows). Phagosomes are indicated (arrowheads). *D–I*, Morphological features of macrophage lipid bodies. In control cell (*D*) and in cells after 1 h of BCG infection (*E* and *F*), lipid bodies were electron-dense structures. At 24 h of infection (*G–I*), lipid bodies were light dense, with a peripheral rim of electron-dense material and an occasional eccentric area (*H*). Interactions between lipid bodies and phagosome (*G*) or between lipid bodies and each other (*I*) were frequently observed. *J*, Lipid body size (diameter) increases drastically during BCG infection. Pleural cells were fixed in a mixture of glutaraldehyde and paraformaldehyde, embedded in agar, and processed for transmission electron microscopy. A total of 35 electron micrographs was randomly taken and analyzed for lipid body diameter measurements. Statistically significant ($p < 0.05$, Student's t tests) differences are indicated by asterisks. Bars, 1 μm.

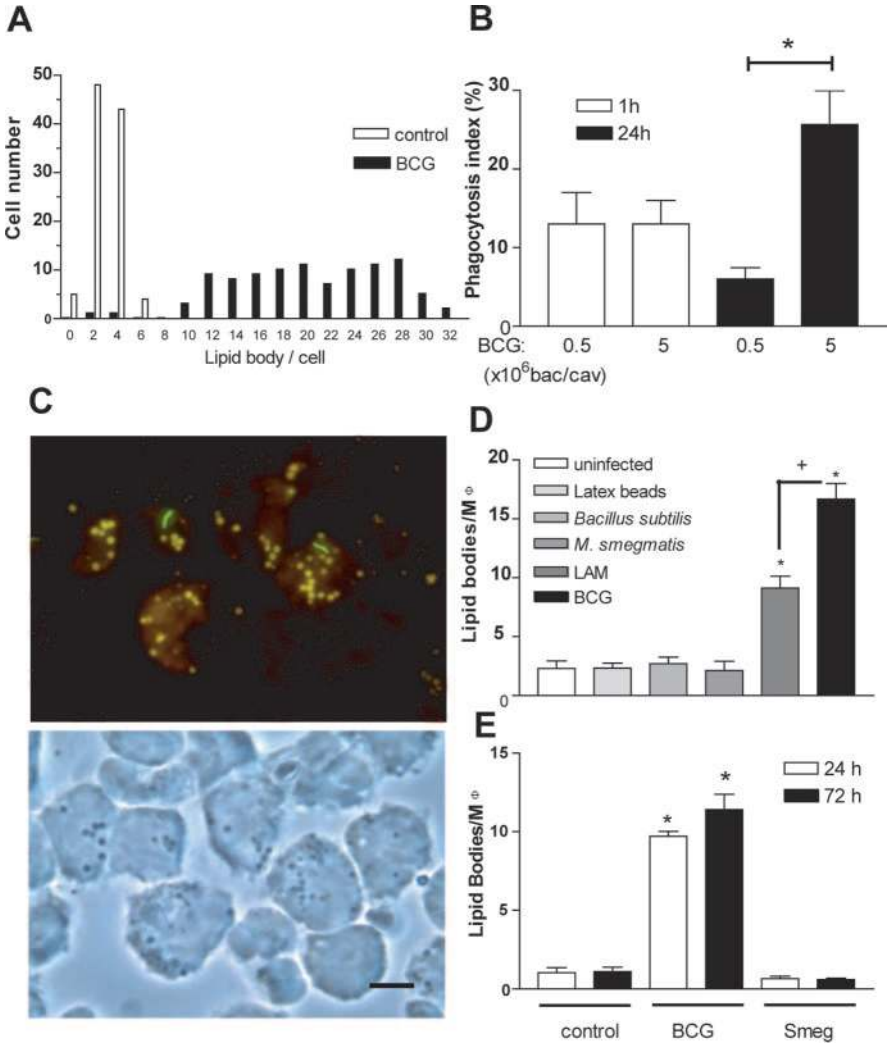

FIGURE 3. Phagocytosis is not essential for lipid body formation after BCG infection. *A*, Lipid bodies per cell from control (□) and infected (5×10^6 bacilli/cavity) groups (■), at 24 h, were enumerated after osmium staining. *B*, Phagocytic index was performed at 1 and 24 h after in vivo infection (5×10^5 or 5×10^6 bacilli/cavity) and analyzed after Kynioun's staining. *C*, *Upper panel*, Fluorescent Nile Red-labeled lipid bodies were visualized at 24 h after in vivo infection as cytoplasmic punctate inclusions (yellow) in macrophages with or without phagocytosed fluorescent labeled BCG (green); *lower panel*, phase contrast of the same cells. Pleural cells were recovered from infected group (5×10^6 bacilli/cavity) at 24 h, fixed with 3.7% formaldehyde, and stained by Nile Red. Bar, 10 μm. *D*, Macrophage lipid bodies from peritoneal cells stimulated in vitro with latex beads (1:1), *B. subtilis* (MOI, 1:1), *M. smegmatis* (MOI, 5:1), LAM (500 ng/ml), and BCG (MOI, 1:1) for 24 h. *E*, Analysis of macrophage lipid bodies from control, BCG-, and *M. smegmatis* (smeg)-infected groups (5×10^6 bacilli/cavity) at 24 and 72 h after infection. Statistically significant ($p < 0.05$) differences between stimulated and control group are indicated by asterisks.

Activation of macrophages with zymosan particles also failed to induce lipid body formation in cells from B6 mice (from 1.67 ± 0.25 in control to 1.93 ± 0.34 lipid bodies/macrophage in zymosan-stimulated cells (mean ± SEM, nonsignificant)).

Interestingly, the mycobacterial cell wall component LAM significantly induced lipid body formation, although not to the same extent as live BCG infection (Fig. 3*D*). Accordingly, i.pl. injection of heat-killed BCG induced a significant increase in the lipid body number at 1 h of infection, and no differences were observed between lipid body induction with live or heat BCG at this time (from 0.82 ± 0.1 lipid bodies/cell in control to 2.93 ± 0.3 lipid bodies/cell after live BCG; 2.54 ± 0.2 lipid bodies/cell in heat-killed BCG). However, after 24 h of infection, live BCG induced more lipid body formation than heat-killed BCG (from 12.1 ± 0.7 to 7.83 ± 0.8 lipid bodies/cell when live and killed BCG were compared), suggesting that lipid body formation was partially dependent of the bacterial viability.

Next, we extend this analysis to compare the lipid body-inducing effect of BCG with a nonpathogenic mycobacteria *M. smegmatis*. As shown in Fig. 3*D*, macrophage stimulation in vitro with *M. smegmatis* (5:1) failed to induce lipid body formation within 24 h, under conditions in which BCG significantly stimulated macrophages to form lipid bodies. Moreover, i.pl. administration of *M. smegmatis* failed to induce lipid body formation in macrophages (or other leukocytes) recovered from the pleural cavity within 24 or 72 h after infection (Fig. 3*E*).

TLR2, but not TLR4, is involved in BCG-induced lipid body formation

In leukocytes, lipid body formation is a highly regulated event that depends on the interaction of cellular receptors with their ligands. The role of TLR-mediated pathogen recognition in the mechanism of lipid body formation was investigated. We observed that BCG-induced lipid body formation in vivo in TLR2-defective B6 mice was drastically inhibited when compared with B6 wild-type mice (Fig. 4*A*). BCG-induced PGE_2 generation was also significantly reduced in $TLR2^{-/-}$ when compared with wild-type mice (H. D'Ávila, unpublished observations). In contrast, TLR4-defective mice from two different strains, C57BL/10 ScCr (Fig. 4*B*) and C3H/HeJ (data not shown), were capable of forming lipid bodies when infected by BCG in vivo, at levels comparable to their TLR4-responsive strains C57BL/10 or C3H/HeN, respectively. The ability of BCG to induce lipid body formation through TLR2-dependent pathway was confirmed in in vitro stimulated peritoneal macrophages. As shown in Fig. 4, *C* and *D*, BCG significantly induced lipid body formation in B6, C57BL/10 ScSn, and C57BL/10 ScCr, but not in $TLR2^{-/-}$ macrophages. Positive control for the TLR knockout experiments was provided, demonstrating that the cells from TLR2 knockout mice retain the capacity to form lipid bodies in response to LPS. Moreover, LAM-induced lipid body formation occurs in a TLR2-dependent manner, adding support to the hypothesis that mycobacterial components were inducing lipid body formation via TLR-dependent pathways (Fig.

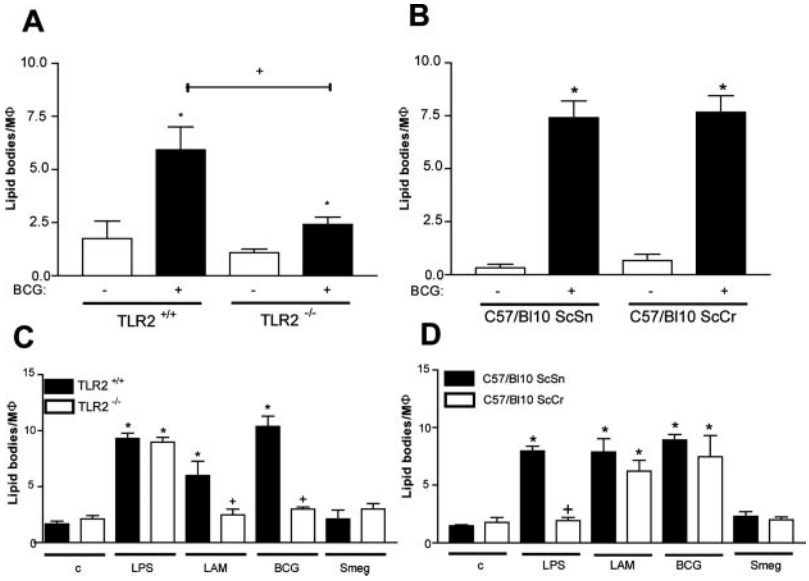

FIGURE 4. Mechanisms involved in lipid body formation induced by BCG in macrophages: role for TLR2 signaling. Analysis of macrophage lipid bodies in wild-type (TLR2$^{+/+}$) and TLR2 knockout (TLR2$^{-/-}$) mice (*A* and *C*), C57BL/10 ScSn (TLR4$^{+/+}$), and C57BL/10 ScCr (TLR4$^{-/-}$) mice (*B* and *D*), 24 h after in vivo BCG infection (*A* and *B*) by 5×10^6 bacilli/cavity or in vitro stimulation (*C* and *D*) by LPS (500 ng/ml), LAM (500 ng/ml), BCG (MOI, 5:1), and *M. smegmatis* (MOI, 5:1). Macrophage lipid bodies were enumerated after osmium staining. Each bar represents the mean ± SEM from 50 consecutively counted macrophages from at least eight animals in in vivo experiments and four independent pools of three animals each in in vitro experiments. Statistically significant ($p < 0.05$) differences between control and infected groups are indicated by asterisks; +, represents differences between wild-type and deficient mice. Mϕ, macrophages.

4*C*). Infection by *M. smegmatis* failed to induce lipid body formation in macrophages from all strains (C57BL6; TLR2$^{-/-}$; C57BL/10 ScSn and C57BL/10 ScCr) analyzed (Fig. 4, *C* and *D*). These results demonstrate a requisite role for TLR2 in BCG recognition and signaling to induce lipid body formation.

Lack of involvement of endogenously generated proinflammatory cytokines in BCG-induced lipid body formation

It has been described previously that cytokines and chemokines may participate in the signaling that leads to lipid body formation (15, 35, 38, 39). The roles of three cytokines/chemokines relevant to macrophage activation in *Mycobacterium*-induced response were evaluated as to their involvement in BCG-induced lipid body formation. As shown in Fig. 5, no difference in BCG-induced lipid body formation was observed 24 h after infection when each respective wild type was compared with TNFRI (Fig. 5*A*), MCP-1/CCL2 (Fig. 5*B*), or IFN-γ (Fig. 5*C*) genetically deficient animals, thus ruling out the involvement of IFN-γ, MCP-1/CCL2, and TNF-α signaling through its receptor type I as endogenous modulators of BCG-induced lipid body formation.

Eicosanoid-forming enzymes localize at lipid bodies

We evaluated whether key eicosanoid-forming enzymes were localized at leukocyte lipid bodies formed within 24 h of BCG infection. Compartmentalization of eicosanoid-forming enzymes, 5-lipoxygenase and COX-2, to lipid bodies was analyzed by immunocytochemistry using conditions of cell fixation and permeabilization that prevented dissolution of lipid bodies. Lipid bodies were visualized by endogenous labeling with the fluorescent fatty acid-containing diglyceride, 1-acyl-2-(7-octyl BODIPY-1-pentanoyl)-*sn*-glycerol (1 μM), for 1 h at 37°C. Fluorescent fatty acid-labeled lipid bodies were visualized as green punctate intracytoplasmic inclusions (Fig. 6, *A* and *B*). Pleural leukocytes stained with anti-COX-2 (Fig. 6*C*) or anti-5-lipoxygenase (data not shown) polyclonal Abs, in addition to perinuclear membrane and cytosolic staining, showed focal punctate cytoplasmic staining that matched with fluorescent labeled lipid bodies. There was no immunoreactivity when control (Fig. 6*D*) normal rabbit serum was used, although fluorescent fatty acid-labeled lipid bodies were strongly visualized.

BCG infection induces eicosanoid generation

Because lipid bodies are stores of the eicosanoid precursor, AA, in different leukocyte subsets, including eosinophils, neutrophils, and monocytes, and contain eicosanoid-forming enzymes (Fig. 6, *A–D*) (40), we investigated whether increased numbers of leukocyte lipid bodies from animals infected by BCG would lead to enhanced PG production. No differences in PGE_2 levels in the pleural wash were observed between control and infected animals after 1 h of BCG infection, but significantly increased levels of PGE_2 in the pleural

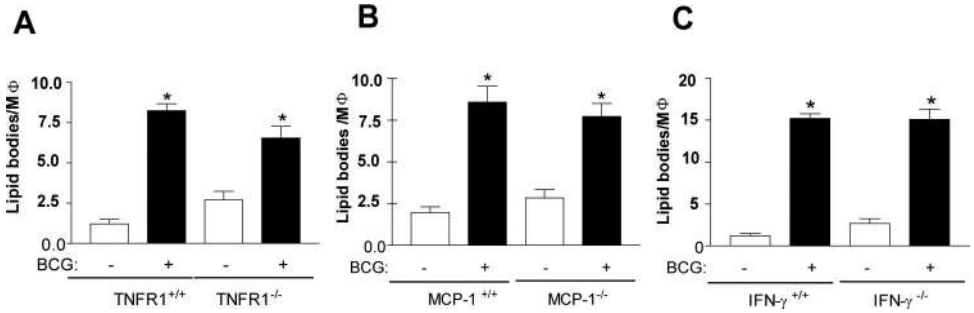

FIGURE 5. Lack of involvement of TNFR1, MCP-1, and IFN-γ in lipid body formation induced by BCG in macrophages. Analysis of macrophage lipid bodies in wild-type (TNFR1$^{+/+}$) and TNFR1 knockout (TNFR1$^{-/-}$) mice (*A*), wild-type (MCP-1$^{+/+}$) and MCP-1 knockout (MCP-1$^{-/-}$) mice (*B*), and wild-type (IFN-$\gamma^{+/+}$) and IFN-γ knockout (IFN-$\gamma^{-/-}$) mice (*C*) 24 h after BCG infection (5×10^6 bacilli/cavity). Macrophage lipid bodies were enumerated after osmium staining. Each bar represents the mean ± SEM from 50 consecutively counted macrophages from at least eight animals. Statistically significant ($p < 0.05$) differences between control and infected groups are indicated by asterisks. Mϕ, macrophages.

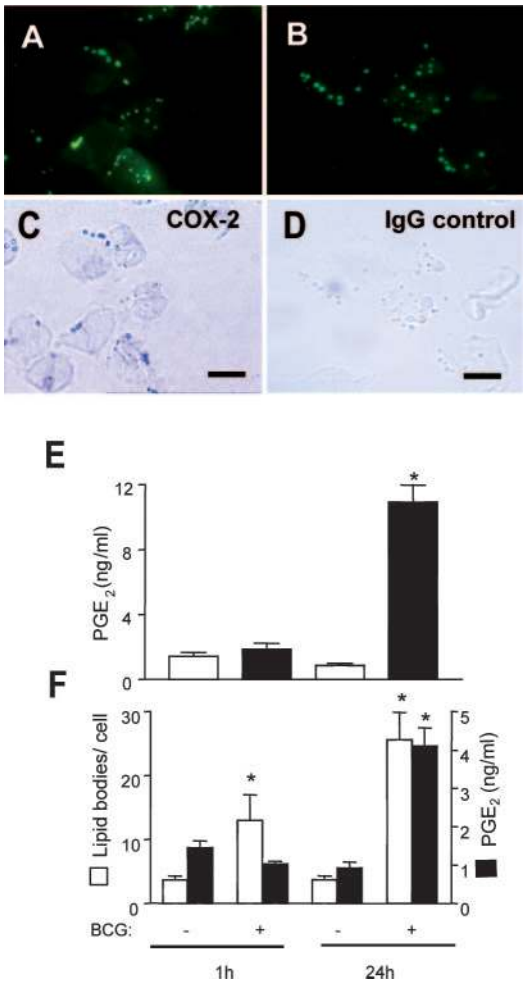

FIGURE 6. BCG infection induces both compartmentalization of COX-2 within lipid bodies and priming for enhanced eicosanoid generation. *A* and *B*, Lipid bodies were visualized by endogenous labeling with fluorescent fatty acid-containing diglyceride, 1-acyl-2-(7-octyl-BODIPY-1-pentanoyl)-*sn*-glycerol (1 μM, for 1 h) as green punctate cytoplasmatic inclusions under FITC excitation. Images of identical fields depict glucose oxidase immunostaining with rabbit anti-COX-2 (*C*) and purified rabbit IgG (*D*) as control using light microscopy in a $\times$100 objective lens from pleural leukocytes obtained 24 h after BCG infection. Bars, 10 μm. *E*, Pleural wash levels of PGE_2 produced during 24 h of i.pl. infection by BCG (5×10^6 bacilli/cavity) in B6 mice. *F*, Animals were i.pl. stimulated with BCG or vehicle for 1 or 24 h for lipid body formation. After that, pleural leukocytes were obtained for lipid body enumeration and leukocytes were washed in Ca^{2+}/Mg^{2+}-free HBSS. Leukocytes (1×10^6 cells/ml) were resuspended in HBSS containing Ca^{2+}/Mg^{2+} and then restimulated with A23187 (0.5 μM) for 15 min. PGE_2 were measured by EIA, and lipid bodies were enumerated following osmium staining. Data are means $\pm$ SEM from at least eight mice. Statistically significant differences ($p < 0.05$) are indicated by asterisks.

fluid were observed after 24 h of infection (Fig. 6*E*), a time characterized by the highest lipid body formation (Fig. 1*E*).

Unstimulated leukocytes respond to submaximal concentrations of calcium ionophore by generating low levels of eicosanoids. In a process known as priming, the cells after in vivo infection with BCG (1 and 24 h) were stimulated with 0.5 μM calcium ionophore A23187. The levels of the PGE_2 released after priming increased only 24 h after infection (Fig. 6*F*), which is in agreement with the time required for COX-2 induction and compartmentalization within lipid bodies.

Lipid bodies are sites for BCG-enhanced PGE_2 synthesis in macrophages

Because BCG infection led to quantitative increases in both lipid body formation and enhanced PGE_2 formation, we hypothesized that lipid bodies were domains for compartmentalized PGE_2 synthesis. To investigate intracellular sites of newly formed PGE_2, we adapted a newly developed strategy for direct in situ immunolocalization of LTC_4 synthesis (35). EDAC was used to cross-link eicosanoid carboxyl groups to amines in adjacent proteins, and immobilized PGE_2 was immunofluorescently detected. ADRP was used as a marker of lipid bodies for colocalization purpose. ADRP is ubiquitously expressed in many cells and tissues as a major component of lipid droplets (41). Recently, we demonstrated that ADRP specifically localizes at lipid bodies within inflammatory leukocytes, including macrophages, indicating that ADRP is a useful leukocyte lipid body marker for colocalization studies (Maya-Monteiro et al., submitted for publication).

Macrophages were the main PG producer cells in BCG-induced inflammatory reaction (data not shown). Macrophages from BCG-, but not vehicle-stimulated mice exhibited a strong localized punctated or ring shape staining for ADRP-labeled lipid bodies (Fig. 7*A*, *left panel*). Macrophages recovered from BCG-infected animals showed intense and punctated immunofluorescent staining for PGE_2 (Fig. 7*A*, *center panel*). As shown in Fig. 7*A*, *right panel*, PGE_2 intracellular site of production perfectly matches ADRP-stained lipid bodies.

The specificity of this immunofluorescent staining for PGE_2 was ascertained. First, the detected PGE_2 should be a product of an active COX pathway; accordingly, indomethacin, which blocks COX activity, completely abolished immunofluorescent staining for PGE_2 (Fig. 7*B*, *central panel*). In addition, specificity of the immunofluorescence for PGE_2 was supported by the absence of immunostaining when an isotype control Ab replaced the anti-PGE_2 mAb (Fig. 7*C*, *center panel*). Moreover, leukocytes from vehicle-stimulated animals exhibited no immunofluorescent staining for PGE_2 (Fig. 7*D*, *central panel*), demonstrating no background staining or preformed PGE_2, as expected in the absence of cell stimulation. These findings validated the specificity for detecting PGE_2 formed at its formation sites within stimulated macrophages, and place lipid bodies as the major localization site for newly formed PGE_2 during the BCG infection.

Inhibition of lipid body formation and PGE_2 production by nonsteroidal anti-inflammatory drugs (NSAIDs) modulates cytokine host response to mycobacterial infection

NSAIDs, including aspirin and NS-398, have been shown previously to inhibit lipid body formation induced by *cis*-unsaturated fatty acids, through COX-independent mechanisms (42, 43). The capacity of aspirin and NS-398 to inhibit BCG-induced lipid body formation was investigated. As shown in Fig. 8*A*, both aspirin (5 μM) and NS-398 (1 μM) drastically inhibited BCG-induced lipid body formation within 24 h. As expected, at the concentrations of NSAIDs used, the BCG-induced PGE_2 generation was completely abrogated (Fig. 8*A*).

As extensively reviewed elsewhere, mycobacterial infection induces increased production of a number of proinflammatory cytokines (including IL-1, TNF-α, IFN-γ, and IL-12), as well as anti-inflammatory ones (including IL-10 and TGF-β), and a tightly controlled balance of cytokine response determines infection outcome, as cytokine response is crucial to the control of the infection, but may also contribute to the chronic infection and associated

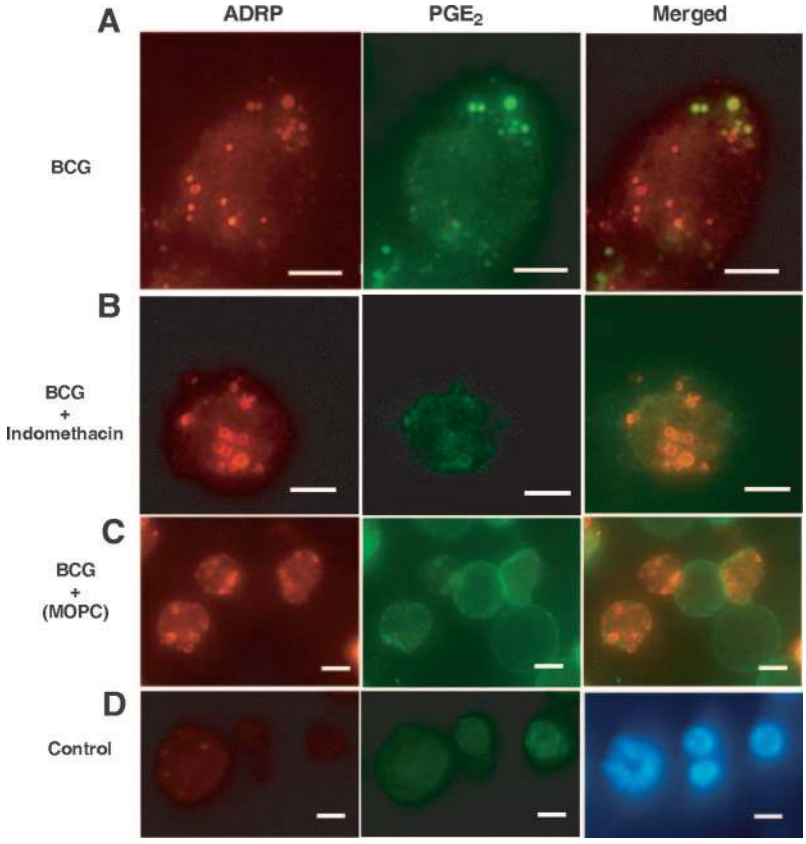

FIGURE 7. Newly formed PGE_2 localizes in ADRP-associated lipid bodies at 24 h of BCG infection. *A*, Macrophages from BCG-infected animals were labeled for ADRP-associated lipid bodies (*left panel*) and for newly formed PGE_2 (*middle panel*). Merged image (*right panel*) showed colocalization of PGE_2 in ADRP-associated lipid bodies. *B*, BCG-infected animals were treated with indomethacin (4 mg/kg) 4 h before the sacrifice. *C*, IgG1 irrelevant isotype (MOPC) was used as control for PGE_2 labeling. *D*, Pleural cells from noninfected animals were negative for both ADRP (*left panel*) and PGE_2 (*middle panel*); the nuclei of control cells are observed after 4′-6-diamidino-2-phenylindole staining (*right panel*). Bars, 10 μm.

pathology (44). To characterize the role of aspirin- and NS-398-induced inhibition of formation of lipid bodies and PGE_2 on mycobacterial host response, the levels of one proinflammatory (TNF-α) and one anti-inflammatory cytokine (IL-10) were investigated. BCG infection of macrophage led to a significant increase in both TNF-α (from 66.3 $\pm$ 15 in noninfected to 297.8 $\pm$ 21.6 pg/ml in BCG-infected macrophages) and IL-10 (from 28.1 $\pm$ 4.9 in noninfected to 66.0 $\pm$ 30.9 pg/ml in BCG-infected macrophages). The effect of aspirin and NS-398 on TNF-α and IL-10 production by BCG-infected macrophages was investigated. As shown in Fig. 8*B*, treatment of BCG-infected macrophages with aspirin or NS-398 led to an increment of BCG-induced TNF-α production of 72 and 29%, respectively, whereas the production of IL-10 simultaneously measured at those same samples was reduced by 81 and 74%, respectively. Collectively, our data suggest that lipid body-derived endogenous PGE_2 down-modulate macrophage response by inhibiting BCG-induced TNF production (cytokine with important roles in mediating macrophage-induced mycobacterial killing) and by increasing the levels of the anti-inflammatory cytokine IL-10.

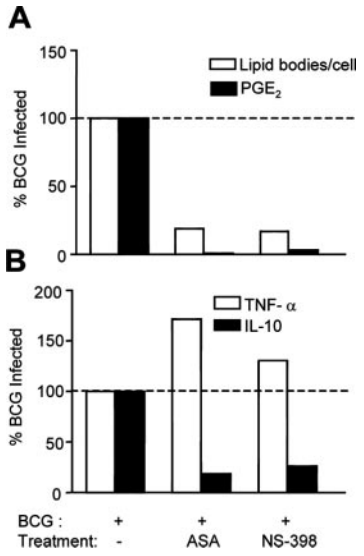

FIGURE 8. NSAIDs, aspirin, and NS-398 inhibit lipid body formation, PGE_2, and IL-10 synthesis, while enhancing TNF-α production induced by BCG. Peritoneal macrophages (1×10^6) were infected in vitro by BCG (MOI, 5:1) for 1 h. Noninternalized BCG were removed, and the cells were treated with 5 μM aspirin (ASA) or 1 μM NS-398 for 24 h at 37°C. Vehicle (0.01% DMSO) was used as control. Results are expressed as percentage of BCG-infected group of: *A*, lipid body formation (□) and PGE_2 synthesis (■); *B*, TNF-α (□) and IL-10 (■) production. Lipid bodies were enumerated after osmium staining, and PGE_2 were measured by EIA. TNF-α and IL-10 were measured simultaneously by multiplex cytokine assay. Results are the mean from three independent pools of three to five animals each.

Discussion

The mechanisms involved in lipid-laden (foamy) macrophage formation and its functional significance have not been addressed previously. In this study, we evaluated the effects of *M. bovis* BCG infection in mice on lipid body formation. We demonstrated that infection-induced foamy-like macrophages were due to compartmentalization of lipids within their cytoplasm in distinct hydrophobic organelles named lipid bodies or lipid droplets. We showed that lipid bodies are dynamic organelles that have their formation highly regulated through TLR2-dependent mechanisms. Moreover, evidence was provided that lipid bodies are functionally active organelles, as both eicosanoid-forming enzymes and newly formed lipid mediator (PGE_2) are colocalized within lipid bodies.

We observed that BCG was capable of inducing a dose- and time-dependent increase on lipid body formation. Lipid body formation initiates very rapidly, and significantly increased lipid body

numbers were noted within 1 h, reached maximum levels within 24 h, and remained increased for at least 15 days after BCG infection. Ultrastructural analysis of leukocytes from infectious foci revealed morphological differences in lipid bodies in the course of infection. Within 1 h of BCG infection, macrophages showed strongly osmiophilic cytoplasmic lipid bodies that, although increased in number, were morphologically similar to lipid bodies from control cells. In contrast, after 24 h of infection, lipid bodies became large and light dense structures with a peripheral rim of electron-dense material, and were frequently observed in close proximity to phagosome-containing bacteria. Those morphological differences may reflect differences in lipid composition and/or ratio neutral lipids/phospholipids within lipid bodies. Typically, increases in lipid body size and numbers are accompanied by accumulation of neutral lipids in their hydrophobic core (10, 45). Indeed, lipid analysis from BCG-infected macrophages demonstrated significant and time-dependent increases in the cellular pool of triglycerides and cholesterol esther (C. Maya-Monteiro, H. D'Avila, and P. Bozza, unpublished observations). However, a contribution of mycobacterial lipids to lipid body biogenesis could not be ruled out. Indeed, intense cell wall mycobacterial trafficking out of mycobacterial phagosome to other organelles within infected macrophages has been demonstrated (46, 47). The identification of lipid composition of BCG-induced lipid bodies is currently under investigation. The electron-dense ring around lipid bodies might represent osmiophilic phospholipids and/or proteins in the periphery of lipid bodies. Indeed, recent studies have shown that lipid bodies are surrounded by a hemi-membrane of unique fatty acid composition (10). Moreover, the surface of BCG-induced lipid bodies was shown to be enriched in the protein ADRP; that is in agreement with previous demonstrations that ADRP is the main surface protein of lipid bodies in different mammalian cells, including leukocytes (41) (C. Maya-Monteiro, W. Yu, P. Bozza, and P. Weller, submitted for publication).

Interestingly, our results indicated that leukocytes do not need to be infected by BCG to have lipid bodies formed, as it was observed that both infected as well as uninfected cells had significantly increased cytoplasmic lipid body numbers, indicating that mechanisms involved in lipid body formation were independent of bacterial ingestion. In addition, macrophage uptake of latex beads and of the nonpathogenic mycobacteria *M. smegmatis* was not able to trigger mechanisms of lipid body formation. Collectively, those findings indicate that phagocytosis is not sufficient nor essential for BCG-induced lipid body formation, and may suggest that transfer of mycobacterial lipids to uninfected bystander cells and/or cytokine and other inflammatory mediators generated at the infection foci might contribute to lipid body formation in leukocytes. Although cytokines and chemokines, including MCP-1/CCL2, were shown to mediate lipid body formation in low density lipoprotein- and allergic-induced inflammation (38, 39), our results using genetically deficient mice suggest that major macrophage-activating cytokines/chemokines, MCP-1/CCL2, IFN-γ, or TNF-α, are not involved in BCG-induced lipid body formation.

Mechanisms involved in BCG-induced lipid body formation were analyzed. Pattern recognition receptors, including mannose receptors, complement receptors, and most importantly TLRs, are critical for sensing of mycobacterial Ags and host cell signaling (48). Different members of the TLR family, including TLR2, TLR4, TLR6, and TLR1, which dimerize with TLR2, have been implicated in mycobacterial Ag recognition (49–51). BCG-induced macrophage lipid body formation was drastically inhibited in TLR2-deficient mice, suggesting a requisite role for TLR2 in this phenomenon. In line with our findings, purified cell wall mycobacterial Ags, including LAM, phosphatidylinositol mannosides, and 19-kDa lipoprotein, all signal through TLR2-dependent pathways (52, 53). Indeed, lipid body formation could also be triggered by the TLR2-ligand LAM, although to a lesser extent than that observed with live BCG infection. In contrast, BCG-induced lipid body formation was not modified when two distinct TLR4 mouse-deficient strains were used. Accordingly, TLR4-deficient mice show normal macrophage recruitment and activation, as well as control the BCG infection (54). Of note, activation of macrophages in vitro with zymosan particles failed to induce lipid body formation, thus suggesting that TLR2 activation, although essential for mycobacterial-induced lipid body formation, is not sufficient to trigger pathways of lipid body formation, and other cofactors may be involved. However, the lack of lipid body-induced response in TLR2 knockouts is not *Mycobacterium* specific, as the pathogenic intracellular parasite *Trypanosoma cruzi* also induces lipid body formation in a TLR2-dependent pathway.

Pertinent to the functions of lipid bodies in leukocytes, lipid bodies are distinct cytoplasmic organelles, functioning both as nonmembrane depot of AA and as intracellular sites for regulated metabolism of arachidonate (40). Of special interest for inflammatory cells in which increased eicosanoid synthesis is observed, lipid body arachidonyl-phospholipids might provide a source of substrate AA without requiring the perturbation of the integrity of membranes and could be replenished from the arachidonyl-triglycerides abundant in lipid bodies (23). In a different perspective, though, lipid bodies could also function as a draining compartment to rapidly uptake and reacetylate free AA with potentially detrimental outcome for the host cell, because it has been demonstrated recently that AA has important functions in inducing apoptosis of *Mycobacterium*-infected macrophages, and in actin recruitment to the phagosome, enabling phagosome maturation, leading to increased mycobacterial killing (4, 24).

The hypothesis that the formation of new lipid bodies elicited by BCG infection provides a distinct intracellular domain for regulated eicosanoid production is supported by different evidence. First, BCG-induced lipid body formation were sites of immunolocalized COX-2. Second, in this study, we observed a significant correlation between lipid body formation and PGE_2 generation in the BCG infection site. Moreover, BCG-driven lipid body-enriched leukocytes were shown to be primed for enhanced PGE_2 production when restimulated by submaximal concentrations of the ionophore A23187, suggesting that lipid bodies are early response structures involved in the production of lipid mediators of inflammation in vivo.

Direct assessment of intracellular sites for eicosanoid has been elusive, as those mediators are newly formed, nonstorable, and rapidly released upon cell stimulation. Recently, a new strategy to cross-link newly formed LTC_4 at its sites of synthesis within stimulated eosinophils was described, enabling the immunofluorescent localization of newly formed LTC_4 at its intracellular formation locale (35, 39). By adapting this technique to investigate intracellular PG synthesis by inflammatory leukocytes in vivo, we were able to demonstrate that pathogen-induced lipid bodies are the main intracellular domain for PGE_2 synthesis. To our knowledge, this is the first direct demonstration of leukocyte intracellular compartmentalization of PG formation in in vivo inflammatory conditions. Together, our findings support a role for lipid bodies to function as specific sites for eicosanoid formation. In accordance, Rangel Moreno et al. (25) have demonstrated recently that foamy macrophages located in pneumonic areas of *M. tuberculosis* infection in mice were strongly positive for COX-2 and PGE_2 synthase staining. The enhanced capacity of macrophages to generate PGE_2 in the course of mycobacterial infection due to increased lipid

body formation and compartmentalization of signaling to eicosanoid production within lipid bodies may contribute to the mechanisms that intracellular pathogens have evolved to survive in host cells. Indeed, high concentration of PGE_2 is a potent inhibitor of Th1-type response and TNF and NO production (55, 56). Accordingly, treatment with aspirin or NS-398 led to an enhancement of TNF-α production and a drastic reduction on IL-10 generation induced by BCG infection, which paralleled the inhibitory effect of these NSAIDs on PGE_2 and lipid body formation. In agreement, increased levels of PGE_2 favor intracellular pathogen growth, a phenomenon that could be reverted by treatment with COX-2 inhibitors (25, 27). Collectively, our data suggest that lipid body-derived endogenous PGE_2 down-modulate macrophage response by inhibiting BCG-induced TNF production (cytokine with important roles in mediating macrophage-induced mycobacterial killing) and increasing the levels of the anti-inflammatory cytokine IL-10. Taken together with the data that, different from *M. bovis* BCG, the fast growing nonpathogenic *M. smegmatis* failed to form lipid bodies suggests that lipid bodies may perhaps have roles in microbial pathogenesis. Further studies will be necessary to establish the role of lipid bodies in the virulence mechanisms of intracellular parasites.

Remarkably, lipid bodies from infected animals were frequently found in close apposition to *Mycobacterium*-containing phagosomes with suggestive images of organelle interactions. Similar lipid body phagosome interactions have been noted in inflammatory macrophages from rats during the infection with the intracellular parasite *T. cruzi* (57). Although the significance of this interaction remains to be elucidated, it raises intriguing possibilities in light of lipid body composition and functions. First, lipidic content of lipid bodies may serve as a carbon source for bacterial growth. Second, recent studies focusing on the protein profile of lipid bodies in different cell types have revealed a broad list of proteins found within lipid bodies, including not only proteins involved in lipid transport and metabolism, but also several small GTPases of the Rab family and kinases; therefore, lipid bodies may have much broader functions than previously recognized, including roles in cellular lipid metabolism, membrane trafficking, intracellular signaling, and cell-to-cell communication (16, 17, 19–21, 58). Of interest, Rab 5, Rab 7, and PI3K, which were shown to be compartmentalized at lipid bodies, are key molecules in the control of sequential interactions of early and late endosomes, and have also been implicated in the maturation process of phagosomes containing intracellular pathogens (59, 60).

In conclusion, BGC induces rapid and persistent leukocyte lipid body formation in a TLR2-dependent mechanism. Leukocyte lipid bodies formed during BCG infection are specialized, inducible intracellular domains that may function as signaling platforms in inflammatory mediator production in the sense that the compartmentalization of substrate and key enzymes within intracellular lipid bodies has direct impact on the capacity of leukocytes to generate increased amounts of eicosanoids. In fact, lipid bodies are the main intracellular site for PGE_2 synthesis during intracellular pathogen infection. Together, our observations suggest that lipid bodies carry out specific functions in eicosanoid generation in the course of intracellular pathogen infection that go beyond those of simple lipid storage organelles and may potentially have implications to the pathogenesis of mycobacterial infection.

Acknowledgments

We are indebted to Dr. Bandeira-Melo and Dr. Viola for helpful comments on the work and the manuscript. We are grateful to Dr. S. Akira (Department of Host Defense, Research Institute for Microbial Disease, Osaka University, Osaka, Japan) and Dr. Gazzinelli (Universidade Federal de Minas Gerais, Belo Horizonte, Minas Gerais, Brazil) for providing the TLR2-deficient mice used in this study. We thank Dr. Barret J. Rollins from the Dana-Farber Cancer Institute (Boston, MA) and Dr. Craig Gerard from the Children's Hospital, Harvard Medical School (Boston, MA), for providing MCP-1-deficient mice. We thank Dr. Pessolani and Dr. Mendonça-Lima for insightful suggestions and reagents. We also thank the Centro de Microscopia Electronica (Universidade Federal de Minas Gerais) for use of its facilities.

Disclosures

The authors have no financial conflict of interest.

References

1. Frieden, T. R., T. R. Sterling, S. S. Munsiff, C. J. Watt, and C. Dye. 2003. Tuberculosis. *Lancet* 362: 887–899.
2. Russell, D. G. 2003. Phagosomes, fatty acids and tuberculosis. *Nat. Cell Biol.* 5: 776–778.
3. Vergne, I., J. Chua, S. B. Singh, and V. Deretic. 2004. Cell biology of *Mycobacterium tuberculosis* phagosome. *Annu. Rev. Cell. Dev. Biol.* 20: 367–394.
4. Anes, E., M. P. Kuhnel, E. Bos, J. Moniz-Pereira, A. Habermann, and G. Griffiths. 2003. Selected lipids activate phagosome actin assembly and maturation resulting in killing of pathogenic mycobacteria. *Nat. Cell Biol.* 5: 793–802.
5. Gatfield, J., and J. Pieters. 2000. Essential role for cholesterol in entry of mycobacteria into macrophages. *Science* 288: 1647–1650.
6. Russell, D. G., H. C. Mwandumba, and E. E. Rhoades. 2002. *Mycobacterium* and the coat of many lipids. *J. Cell Biol.* 158: 421–426.
7. Ridley, D. S., and M. J. Ridley. 1987. Rationale for the histological spectrum of tuberculosis: a basis for classification. *Pathology* 19: 186–192.
8. Cardona, P. J., R. Llatjos, S. Gordillo, J. Diaz, I. Ojanguren, A. Ariza, and V. Ausina. 2000. Evolution of granulomas in lungs of mice infected aerogenically with *Mycobacterium tuberculosis*. *Scand. J. Immunol.* 52: 156–163.
9. Hernandez-Pando, R., L. Pavon, K. Arriaga, H. Orozco, V. Madrid-Marina, and G. Rook. 1997. Pathogenesis of tuberculosis in mice exposed to low and high doses of an environmental mycobacterial saprophyte before infection. *Infect. Immun.* 65: 3317–3327.
10. Tauchi-Sato, K., S. Ozeki, T. Houjou, R. Taguchi, and T. Fujimoto. 2002. The surface of lipid droplets is a phospholipid monolayer with a unique fatty acid composition. *J. Biol. Chem.* 277: 44507–44512.
11. Murphy, D. J. 2001. The biogenesis and functions of lipid bodies in animals, plants and microorganisms. *Prog. Lipid Res.* 40: 325–438.
12. Van Meer, G. 2001. Caveolin, cholesterol, and lipid droplets? *J. Cell Biol.* 152: F29–F34.
13. Dvorak, A. M., P. F. Weller, V. S. Harvey, E. S. Morgan, and H. F. Dvorak. 1993. Ultrastructural localization of prostaglandin endoperoxide synthase (cyclooxygenase) to isolated, purified fractions of guinea pig peritoneal macrophage and line 10 hepatocarcinoma cell lipid bodies. *Int. Arch. Allergy Immunol.* 101: 136–142.
14. Bozza, P. T., W. Yu, J. F. Penrose, E. S. Morgan, A. M. Dvorak, and P. F. Weller. 1997. Eosinophil lipid bodies: specific, inducible intracellular sites for enhanced eicosanoid formation. *J. Exp. Med.* 186: 909–920.
15. Bozza, P. T., W. Yu, J. Cassara, and P. F. Weller. 1998. Pathways for eosinophil lipid body induction: differing signal transduction in cells from normal and hypereosinophilic subjects. *J. Leukocyte Biol.* 64: 563–569.
16. Yu, W., P. T. Bozza, D. M. Tzizik, J. P. Gray, J. Cassara, A. M. Dvorak, and P. F. Weller. 1998. Co-compartmentalization of MAP kinases and cytosolic phospholipase A_2 at cytoplasmic arachidonate-rich lipid bodies. *Am. J. Pathol.* 152: 759–769.
17. Yu, W., J. Cassara, and P. F. Weller. 2000. Phosphatidylinositide 3-kinase localizes to cytoplasmic lipid bodies in human polymorphonuclear leukocytes and other myeloid-derived cells. *Blood* 95: 1078–1085.
18. Umlauf, E., E. Csaszar, M. Moertelmaier, G. J. Schuetz, R. G. Parton, and R. Prohaska. 2004. Association of stomatin with lipid bodies. *J. Biol. Chem.* 279: 23699–23709.
19. Fujimoto, Y., H. Itabe, J. Sakai, M. Makita, J. Noda, M. Mori, Y. Higashi, S. Kojima, and T. Takano. 2004. Identification of major proteins in the lipid droplet-enriched fraction isolated from the human hepatocyte cell line HuH7. *Biochim. Biophys. Acta* 1644: 47–59.
20. Liu, P., Y. Ying, Y. Zhao, D. I. Mundy, M. Zhu, and R. G. Anderson. 2004. Chinese hamster ovary K2 cell lipid droplets appear to be metabolic organelles involved in membrane traffic. *J. Biol. Chem.* 279: 3787–3792.
21. Brasaemle, D. L., G. Dolios, L. Shapiro, and R. Wang. 2004. Proteomic analysis of proteins associated with lipid droplets of basal and lipolytically stimulated 3T3–L1 adipocytes. *J. Biol. Chem.* 279: 46835–46842.
22. Weller, P. F., S. W. Ryeom, S. T. Picard, S. J. Ackerman, and A. M. Dvorak. 1991. Cytoplasmic lipid bodies of neutrophils: formation induced by *cis*-unsaturated fatty acids and mediated by protein kinase C. *J. Cell Biol.* 113: 137–146.
23. Johnson, M. M., B. Vaughn, M. Triggiani, D. D. Swan, A. N. Fonteh, and F. H. Chilton. 1999. Role of arachidonyl triglycerides within lipid bodies in eicosanoid formation by human polymorphonuclear cells. *Am. J. Respir. Cell Mol. Biol.* 21: 253–258.
24. Duan, L., H. Gan, J. Arm, and H. G. Remold. 2001. Cytosolic phospholipase A_2 participates with TNF-α in the induction of apoptosis of human macrophages infected with *Mycobacterium tuberculosis* H37Ra. *J. Immunol.* 166: 7469–7476.

25. Rangel Moreno, J., I. Estrada Garcia, M. De La Luz Garcia Hernandez, D. Aguilar Leon, R. Marquez, and R. Hernandez Pando. 2002. The role of prostaglandin E_2 in the immunopathogenesis of experimental pulmonary tuberculosis. *Immunology* 106: 257–266.
26. Bafica, A., C. A. Scanga, C. Serhan, F. Machado, S. White, A. Sher, and J. Aliberti. 2005. Host control of *Mycobacterium tuberculosis* is regulated by 5-lipoxygenase-dependent lipoxin production. *J. Clin. Invest.* 115: 1601–1606.
27. Freire-de-Lima, C. G., D. O. Nascimento, M. B. Soares, P. T. Bozza, H. C. Castro-Faria-Neto, F. G. de Mello, G. A. DosReis, and M. F. Lopes. 2000. Uptake of apoptotic cells drives the growth of a pathogenic trypanosome in macrophages. *Nature* 403: 199–203.
28. Takeuchi, O., K. Hoshino, T. Kawai, H. Sanjo, H. Takada, T. Ogawa, K. Takeda, and S. Akira. 1999. Differential roles of TLR2 and TLR4 in recognition of Gram-negative and Gram-positive bacterial cell wall components. *Immunity* 11: 443–451.
29. Lu, B., B. J. Rutledge, L. Gu, J. Fiorillo, N. W. Lukacs, S. L. Kunkel, R. North, C. Gerard, and B. J. Rollins. 1998. Abnormalities in monocyte recruitment and cytokine expression in monocyte chemoattractant protein 1-deficient mice. *J. Exp. Med.* 187: 601–608.
30. Benévolo-de-Andrade, T. C., R. Monteiro-Maia, C. Cosgrove, and L. R. R. Castello-Branco. 2005. BCG Moreau Rio de Janeiro: an oral vaccine against tuberculosis. *Mem. Inst. Oswaldo Cruz* 100: 459–465.
31. Karnovsky, M. J. 1965. A formaldehyde-glutaraldehyde fixative of high osmolarity for use in electron microscopy. *J. Cell Biol.* 27: 137A–138A.
32. Bozza, P. T., J. L. Payne, J. L. Goulet, and P. F. Weller. 1996. Mechanisms of platelet-activating factor-induced lipid body formation: requisite roles for 5-lipoxygenase and de novo protein synthesis in the compartmentalization of neutrophil lipids. *J. Exp. Med.* 183: 1515–1525.
33. Lavallee, P. W. 1973. A new fluorescence and Kinyoun's acid-fast stain. *Am. J. Clin. Pathol.* 60: 428–429.
34. Liu, L. X., J. E. Buhlmann, and P. F. Weller. 1992. Release of prostaglandin E_2 by microfilariae of *Wuchereria bancrofti* and *Brugia malayi*. *Am. J. Trop. Med. Hyg.* 46: 520–523.
35. Bandeira-Melo, C., M. Phoofolo, and P. F. Weller. 2001. Extranuclear lipid bodies, elicited by CCR3-mediated signaling pathways, are the sites of chemokine-enhanced leukotriene C_4 production in eosinophils and basophils. *J. Biol. Chem.* 276: 22779–22787.
36. Menezes-de-Lima-Junior, O., E. Werneck-Barroso, R. S. Cordeiro, and M. G. Henriques. 1997. Effects of inhibitors of inflammatory mediators and cytokines on eosinophil and neutrophil accumulation induced by *Mycobacterium bovis* bacillus Calmette-Guerin in mouse pleurisy. *J. Leukocyte Biol.* 62: 778–785.
37. Penido, C., A. Vieira-de-Abreu, M. T. Bozza, H. C. Castro-Faria-Neto, and P. T. Bozza. 2003. Role of monocyte chemotactic protein-1/CC chemokine ligand 2 on γδ T lymphocyte trafficking during inflammation induced by lipopolysaccharide or *Mycobacterium bovis* bacille Calmette-Guerin. *J. Immunol.* 171: 6788–6794.
38. Silva, A. R., E. F. de Assis, L. F. Caiado, G. K. Marathe, M. T. Bozza, T. M. McIntyre, G. A. Zimmerman, S. M. Prescott, P. T. Bozza, and H. C. Castro-Faria-Neto. 2002. Monocyte chemoattractant protein-1 and 5-lipoxygenase products recruit leukocytes in response to platelet-activating factor-like lipids in oxidized low-density lipoprotein. *J. Immunol.* 168: 4112–4120.
39. Vieira-de-Abreu, A., E. F. Assis, G. S. Gomes, H. C. Castro-Faria-Neto, P. F. Weller, C. Bandeira-Melo, and P. T. Bozza. 2005. Allergic challenge-elicited lipid bodies compartmentalize in vivo leukotriene C_4 synthesis within eosinophils. *Am. J. Respir. Cell Mol. Biol.* 33: 254–261.
40. Bozza, P. T., and C. Bandeira-Melo. 2005. Mechanisms of leukocyte lipid body formation and function in inflammation. *Mem. Inst. Oswaldo Cruz* 100: 113–120.
41. Heid, H. W., R. Moll, I. Schwetlick, H. R. Rackwitz, and T. W. Keenan. 1998. Adipophilin is a specific marker of lipid accumulation in diverse cell types and diseases. *Cell Tissue Res.* 294: 309–321.
42. Bozza, P. T., J. L. Payne, S. G. Morham, R. Langenbach, O. Smithies, and P. F. Weller. 1996. Leukocyte lipid body formation and eicosanoid generation: cyclooxygenase-independent inhibition by aspirin. *Proc. Natl. Acad. Sci. USA* 93: 11091–11096.
43. Bozza, P. T., P. Pacheco, W. Yu, and P. F. Weller. 2002. NS-398: cyclooxygenase-2 independent inhibition of leukocyte priming for lipid body formation and enhanced leukotriene generation. *Prostaglandins Leukotrienes Essent. Fatty Acids* 67: 237–244.
44. Flynn, J. L., and J. Chan. 2001. Immunology of tuberculosis. *Annu. Rev. Immunol.* 19: 93–129.
45. Triggiani, M., A. Oriente, G. de Crescenzo, G. Rossi, and G. Marone. 1995. Biochemical functions of a pool of arachidonic acid associated with triglycerides in human inflammatory cells. *Int. Arch. Allergy Immunol.* 107: 261–263.
46. Beatty, W. L., E. R. Rhoades, H. J. Ullrich, D. Chatterjee, J. E. Heuser, and D. G. Russell. 2000. Trafficking and release of mycobacterial lipids from infected macrophages. *Traffic* 1: 235–247.
47. Beatty, W. L., H. J. Ullrich, and D. G. Russell. 2001. Mycobacterial surface moieties are released from infected macrophages by a constitutive exocytic event. *Eur. J. Cell Biol.* 80: 31–40.
48. Doherty, T. M., and M. Arditi. 2004. TB, or not TB: that is the question: does TLR signaling hold the answer? *J. Clin. Invest.* 114: 1699–1703.
49. Sugawara, I., H. Yamada, C. Li, S. Mizuno, O. Takeuchi, and S. Akira. 2003. Mycobacterial infection in TLR2 and TLR6 knockout mice. *Microbiol. Immunol.* 47: 327–336.
50. Takeuchi, O., S. Sato, T. Horiuchi, K. Hoshino, K. Takeda, Z. Dong, R. L. Modlin, and S. Akira. 2002. Cutting edge: role of Toll-like receptor 1 in mediating immune response to microbial lipoproteins. *J. Immunol.* 169: 10–14.
51. Wieland, C. W., S. Knapp, S. Florquin, A. F. de Vos, K. Takeda, S. Akira, D. T. Golenbock, A. Verbon, and T. van der Poll. 2004. Non-mannose-capped lipoarabinomannan induces lung inflammation via Toll-like receptor 2. *Am. J. Respir. Crit. Care Med.* 170: 1367–1374.
52. Means, T. K., S. Wang, E. Lien, A. Yoshimura, D. T. Golenbock, and M. J. Fenton. 1999. Human Toll-like receptors mediate cellular activation by *Mycobacterium tuberculosis*. *J. Immunol.* 163: 3920–3927.
53. Lien, E., T. J. Sellati, A. Yoshimura, T. H. Flo, G. Rawadi, R. W. Finberg, J. D. Carroll, T. Espevik, R. R. Ingalls, J. D. Radolf, and D. T. Golenbock. 1999. Toll-like receptor 2 functions as a pattern recognition receptor for diverse bacterial products. *J. Biol. Chem.* 274: 33419–33425.
54. Fremond, C. M., D. M. Nicolle, D. S. Torres, and V. F. Quesniaux. 2003. Control of *Mycobacterium bovis* BCG infection with increased inflammation in TLR4-deficient mice. *Microbes Infect.* 5: 1070–1081.
55. Betz, M., and B. S. Fox. 1991. Prostaglandin E_2 inhibits production of Th1 lymphokines but not of Th2 lymphokines. *J. Immunol.* 146: 108–113.
56. Renz, H., J. H. Gong, A. Schmidt, M. Nain, and D. Gemsa. 1988. Release of tumor necrosis factor-α from macrophages: enhancement and suppression are dose-dependently regulated by prostaglandin E_2 and cyclic nucleotides. *J. Immunol.* 141: 2388–2393.
57. Melo, R. C., H. D'Avila, D. L. Fabrino, P. E. Almeida, and P. T. Bozza. 2003. Macrophage lipid body induction by Chagas disease in vivo: putative intracellular domains for eicosanoid formation during infection. *Tissue Cell* 35: 59–67.
58. Imanishi, Y., V. Gerke, and K. Palczewski. 2004. Retinosomes: new insights into intracellular managing of hydrophobic substances in lipid bodies. *J. Cell Biol.* 166: 447–453.
59. Via, L. E., D. Deretic, R. J. Ulmer, N. S. Hibler, L. A. Huber, and V. Deretic. 1997. Arrest of mycobacterial phagosome maturation is caused by a block in vesicle fusion between stages controlled by rab5 and rab7. *J. Biol. Chem.* 272: 13326–13331.
60. Fratti, R. A., J. M. Backer, J. Gruenberg, S. Corvera, and V. Deretic. 2001. Role of phosphatidylinositol 3-kinase and Rab5 effectors in phagosomal biogenesis and mycobacterial phagosome maturation arrest. *J. Cell Biol.* 154: 631–644.